Design Optimizations Regarding Eddy Currents of a High Performance Head Gradient Coil

Silke M. Lechner-Greite[1], Jean-Baptiste Mathieu[2], Seung-Kyun Lee[3], Bruce C. Amm[4], Thomas K. Foo[5], John F. Schenck[6], Matt A. Bernstein[7], and John Huston[7]
[1]*Diagnostics and Biomedical Technologies, GE Global Research Europe, Garching n. Munich, Germany,* [2]*Electromagnetics & Superconductivity Laboratory, GE Global Research Niskayuna, Albany, NY, United States,* [3]*MRI Laboratory, GE Global Research Niskayuna, Albany, NY, United States,* [4]*Biomedical and Electronic Systems Laboratory, GE Global Research Niskayuna, Albany, NY, United States,* [5]*Diagnostics and Biomedical Technologies, GE Global Research Niskayuna, Albany, NY, United States,* [6]*MRI Technologies & Systems, GE Global Research Niskayuna, Albany, NY, United States,* [7]*Mayo Clinic, Rochester, MN, United States*

Introduction: Specialty MRI systems for head imaging have shown benefits in neuroimaging due to strong gradient amplitudes and high slew rates [1, 2]. In order for a dedicated head gradient to perform better than whole body gradients in terms of strength and slew rate, while maintaining comparable linearity and reduced forces and torques, the gradient coil must also meet a stringent design target to limit eddy currents and their impact on image quality. In this work, we report on design phase simulation of the eddy current which is induced in the cryostat of a dedicated head magnet. Design phase prediction capability allows the optimization and minimization of linear- and higher-order eddy currents induced in the conducting structures of the cryostat. To accurately simulate experimental assessment during prototype staging (i.e. using an eddy current field camera [3, 4] where the gradient system is modeled as a linear response system), the harmonic response was calculated within finite element simulation and used for amplitude and time constant tracking. Accordingly, the spatial deformations of the gradient field due to eddy currents and their higher-order terms, as well as their decay behavior over time were extracted in transient and frequency domain. This information can be transferred into an image quality prediction model [5] for diffusion weighted imaging as key application for head only systems.

$$g_{ec}(t) = -\frac{dg(t)}{dt} \otimes e(t) \quad (1)$$

$$e(t) = \sum_i \alpha_i \exp^{-t/\tau_i} \quad (2)$$

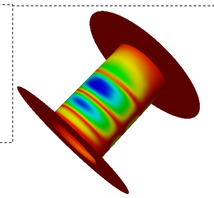

Fig.1: Illustration of the predicted eddy current stream function induced on the thermal shield by the x-gradient coil.

Materials and Methods: The dedicated head system was designed to achieve maximum gradient field strength up to 88 mT/m and a slew rate of 630 T/m/s. Within a 26 cm imaging field of view, a linearity constraint of 16.9% was targeted to achieve comparable performance to conventional gradient coils. The z-gradient coil is based on a symmetric design, whereas the transverse axes x- and y- are asymmetric [6]. Higher-order eddy current harmonic coefficients were constrained, where especially the linear and the third-order were targeted to 1% of the static field harmonics. This was achieved by approximating the thermal shield as a perfect conductor that blocks any normal impinging field from the gradient coil. As such, the spherical harmonics of the magnetic flux density generated by the shield is calculated as a ratio to the harmonics generated by the gradient coil itself (Fig.1). In dynamic simulation, both harmonic and transient responses of the thermal shield were evaluated. Finite element simulations (Maxwell3D, Ansys, Canonsburg, USA) were utilized in time and frequency domain to compare the ideal field map with the eddy current-distorted map in terms of non-linearity and transient response. A frequency analysis at 2 kHz including a thermal shield (conductivity = 5.8×10^7S/m) was performed for all three axes. Field responses of ideal and distorted fields were expressed as the percentage of the applied gradient field. Transient simulations were performed for the x-gradient coil and the thermal shield simulating a trapezoidal pulse with a gradient strength of 82.5mT/m. The total pulse duration was 2 s; the ramp time was 10 us with a sampling rate of 4 us (Fig.2). The simulation was performed in static transient mode as well as frequency transient mode. The residual eddy current effect was extracted and fitted with a linear least square method to (1) with (2) [7] to obtain eddy current amplitude and timing constants. Field maps extracted at the iso-center of the x-gradient coil illustrate the impact of higher-order eddy currents on field linearity and their decay time behavior as a function of time.

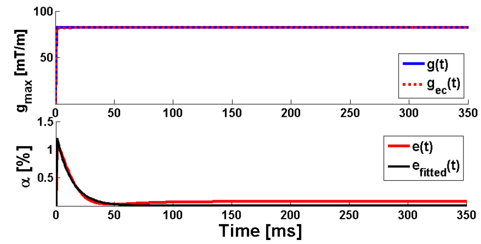

Fig.2: The x-gradient is pulsed with a trapezoidal pulse in simulation. Ideal (g(t)) and eddy current distorted linear term (g_{ec}(t)) are shown. The eddy current time constant is extracted from the difference curve of ideal and eddy response.

Results: The harmonic eddy current analysis showed for constant, linear and higher-order terms an eddy current effect of less than 2%, and about 4% on the second-order harmonic for the x- and y- gradient. All harmonic order components could be designed to be less than 0.5% for the z-gradient (Fig.3). The frequency analysis within finite element simulations resulted in a 1.37% eddy current effect on the pulsed x-gradient representing the maximum eddy current field response of the linear term. This nicely matched the result given in the eddy image design in Fig.3. The fitting of the transient curve given in Fig.2 resulted in eddy current amplitude of 1.39% nicely correlating with the 1.37% of the 2 kHz analysis. A time decay constant of 13.02 ms for the linear term was extracted. The field maps obtained within the transient simulation are summarized in Fig.4. Fig.4a) shows the static field map on the 26 cm sphere assuming no eddy currents induced in the thermal shield. Fig.4b) shows the field map after 1.2 ms including the eddy current field response due to the thermal shield. The difference of the two field maps at 1.2 ms (Fig.4c)) clearly shows the impact of the second-order harmonic on the linearity. Similar difference plots are given in Fig.4d)-f) showing time steps at 12 ms, 24 ms, and 96 ms, respectively. After 96 ms, the second-order influence decayed fully.

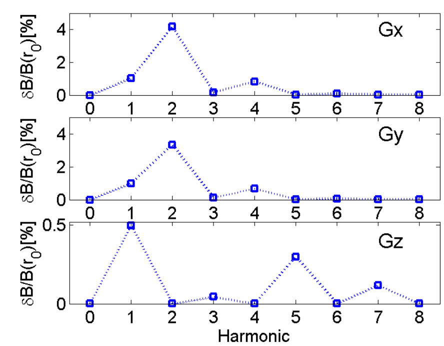

Fig.3: Harmonic analysis of the eddy image field of the head gradient coil for all three axes. The plots show the max. eddy current field strengths immediately following a nominal gradient pulse of 85mT/m within a 26cm spherical volume of interest. The eddy current field is expressed as the percentage of the applied gradient field at r0 = 13 cm.

Discussion and Conclusion: Eddy currents can have a strong influence on image quality. Its inclusion as a constraint in the gradient design phase as a method of predicting image quality, are highly desired. Eddy current field predictions produced in a new head-only gradient design have been evaluated. Constant, linear- and higher-order terms have been targeted within the design optimization phase. The predictions have been validated in finite element simulations which showed excellent agreement in static and frequency simulations compared to the optimization target. The transient analysis provided insight into the temporal decay rates for the linear eddy current term. Future work will include the extraction of the time constants of higher-order terms, and the modeling of image quality using eddy current field responses over time. The developed modeling tools allow the establishment of design specifications for each order of the eddy current harmonics for new gradient coils. For the specific head-only prototype design, the second-order harmonic is expected to substantially influence image quality. With approach described, the design constraints can be further tightened and refined in the subsequent design iterations to ensure optimal image quality. Currently, eddy current data are directly transferred into an imaging model for the evaluation and prediction of image quality. Further expansion of the modeling tools will focus on a frequency sweep solving approach to speed up simulation times.

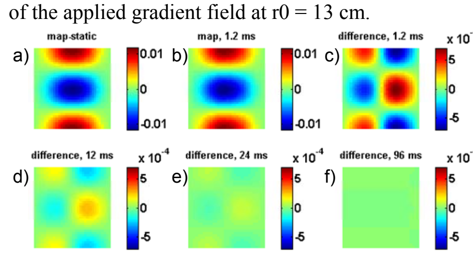

Fig.4: Even-order eddy currents and their impact on linearity as a function of time are in good agreement with the eddy image design (Fig.3). The horizontal and vertical axes show the polar and azimuthal angle covering the entire spherical surface in 32 and 36 steps, respectively. The field is given in T.

Acknowledgment: This work was partly supported by the NIH grant 5R01EB010065.

References:[1]Turner R et al., MRM, 11:903-920 (1993) [2]Chronik B et al., MRM 44:955-963 (2000) [3]Barmet C et al., MRM 60:187–197 (2008) [4]deZanche N et al., MRM 60:176–186 (2008) [5]Lechner S, PhD Thesis (2010), [6]Mathieu JB et al. submitted to ISMRM'12 [7]Bernstein MA, King KF, Zhou XJ, Handbook of MRI Pulse Sequences (2004).